Impact of redox evolution of layered double hydroxides on the immobilization of structural and adsorbed heavy metals

Mengyao Yuan, Minwang Laipan*, Min Zhang, Xueya Wan, Ziyu Wang, Junkang Guo

School of Environmental Science and Engineering, Shaanxi University of Science and Technology, Xi'an 710021, China

* Corresponding author

Dr. Minwang Laipan, E-mail: laipanminwang@sust.edu.cn; Tel: +86 2986132765

This is a 'preproof' accepted article for Mineralogical Magazine. This version may be subject to change during the production process.
DOI: 10.1180/mgm.2024.61

Abstract

In the soil environment, divalent heavy metal ions often interact with trivalent metal ions to form hydrotalcite supergroup nano-minerals (also known as natural layered double hydroxides, LDH), effectively immobilizing heavy metals within the minerals structure. Concurrently, these LDH minerals also show high surface reactivity that can adsorb surrounding heavy metal ions, playing a significant role in the heavy metal pollution purification. However, the impact of the subsequent geochemical evolution of heavy metal-containing LDH on the migration and transformation of structural and surface-adsorbed heavy metals as well as its surface reactivity toward surrounding heavy metals remains unclear. Herein, Ni(II)Fe(III)-LDH and Co(II)Al(III)-LDH were taken as examples to reveal the influence of redox evolution on the immobilization of structural and adsorbed heavy metals . The results of this work indicated that the oxidative-reductive alternating evolution of structural Ni, Fe, and Co elements constrained the transformation of heavy metals, as well as their bioavailability greatly. The oxidative-reductive alternating evolution helped reduce the content of bioavailable heavy metals in exchangeable and carbonate-bounded states. It can also enhance the integration of heavy metals with LDH structure and help transform heavy metals into residual states, thereby reducing their mobility and bioavailability. However, oxidative-reductive evolution significantly reduced the surface reactivity of LDH, diminishing its interface locking ability for surrounding heavy metal ions. This research provides foundational data for assessing the long-term environmental performance of LDH.

https://doi.org/10.1180/mgm.2024.61 Published online by Cambridge University Press

Keywords: Layered double hydroxides; heavy metals; Nano-minerals; Geochemical evolution; migration and transformation

https://doi.org/10.1180/mgm.2024.61 Published online by Cambridge University Press

1. Introduction

With the rapid development of industrialization and urbanization, soil heavy metal pollution has become an increasingly prominent environmental issue (Liu et al., 2022, Qiu et al., 2022). In China, nearly 20 million hectares of farmland are affected by heavy metals, accounting for about one-fifth of the total arable land (Sodango et al., 2018). Addressing soil heavy metal pollution has become an urgent problem, and varied methods have been developed for heavy metals immobilization and extraction, including adsorption (Muhammad et al., 2021, Haris et al., 2022, Zhang et al., 2022), precipitation (Zhou et al., 2010, Xu et al., 2023), ion exchange (Guo et al., 2021, Qiu et al. 2022), solvent extraction (de Souza E Silva et al., 2006), membrane separation (Ahmad et al., 2022), electrochemical means (Wang et al., 2022a) and biological approaches (Guo et al., 2020, Liu et al., 2024). It's believed that soil minerals play a unique role in controlling pollution, as they can adsorb and immobilize heavy metal ions (Zhu et al., 2016, Wang et al., 2022b, Liu et al. 2024); more importantly, some minerals can lock heavy metals within their lattice, effectively reducing the mobility and bioavailability of heavy metal ions (Siebecker et al., 2018, Laipan et al., 2024). Heavy metal ions may engage in the mineral formation process once they enter the soil; therefore, studies with a particular emphasis on the interaction between soil mineral particles or free metal ions and heavy metal ions have become the focus of research (Siebecker et al. 2018).

In recent years, the interaction of divalent heavy metal ions with metal oxides or clay minerals in soil to form layered double hydroxides (LDH) supergroup nano-

https://doi.org/10.1180/mgm.2024.61 Published online by Cambridge University Press

minerals has emerged as a new hot topic (Siebecker et al. 2018). LDH, including hydrotalcite and hydrotalcite-like minerals, are primarily composed of divalent and trivalent metal hydroxides (Yu et al., 2017, Laipan et al., 2020). The main reason for the interest in LDH supergroup minerals in soil is that divalent heavy metal ions can readily form LDH minerals with widely present Al^{3+}/Fe^{3+} or Al^{3+}/Fe^{3+}-containing soil minerals in aqueous media, achieving the fixation of heavy metals within the LDH lattice (Peltier et al., 2010, Zhu and Elzinga 2014, Aucour et al., 2015, Laipan et al. 2024). Concurrently, the high surface reactivity of LDH nano minerals plays a significant role in the adsorption of heavy metals (Liang et al., 2013, He et al., 2018, Laipan et al., 2023). Thus, LDH play a critical role in heavy metals immobilization both by adsorption and lattice fixation in soil environment. But one concern here is whether LDH can immobilize surface adsorbed and lattice-fixed heavy metals chronically or permanently. It depends on the variation of LDH's stability and surface reactivity during the long-term geochemical evolution in soil environment. Due to the complexity of soil environment, the geochemical evolution processes of LDH occur inevitably. The natural LDH, especially those heavy metal-bearing LDH mostly contain metal elements (e.g., Cu, Co, Ni, Fe, etc.) that can be reduced or oxidized in the environment by reducing and oxidizing substances/species (such as reducing organic matter, photo-generated electrons/holes, surface active oxygen species, etc.) (Laipan et al. 2020). Therefore, it is likely that heavy metal-bearing LDH may undergo alternating oxidation and reduction evolution processes. However, there is insufficient understanding of the variation of stability and surface reactivity of heavy metal-bearing LDH minerals

https://doi.org/10.1180/mgm.2024.61 Published online by Cambridge University Press

during subsequent geochemical evolution processes in soil environment, as well as the potential re-migration and transformation behaviors of heavy metals in these minerals.

To examine the impact of oxidation-reduction alternating evolution on the structural stability, surface reactivity, heavy metal locking performance, and heavy metal re-migration and transformation behaviors of heavy metal-bearing LDH, CoAl-LDH and NiFe-LDH were used as representatives. By repeatedly altering the valence states of structural Co and Fe in LDH, this study investigated how the redox evolution affects the structure of LDH, the state of heavy metal existence, the migration and transformation of heavy metals, and the variation of adsorption performance of LDH to heavy metal. The findings provide experimental evidence for assessing the long-term performance of LDH in heavy metals immobilization.

2. Materials and Methods

2.1 Synthesis of LDH

Using metal nitrates as starting materials, CoAl-LDH and NiFe-LDH containing divalent heavy metal ions (Co(II) and Ni(II)) were synthesized through conventional co-precipitation methods (Laipan et al. 2023, Laipan et al. 2024), with a molar ratio of divalent to trivalent ions of 2:1. For CoAl-LDH synthesis, a 500 mL solution of $Co(NO_3)_2 \cdot 6H_2O$ (0.1 mol/L) and $Al(NO_3)_3 \cdot 9H_2O$ (0.05 mol/L) and a 500 mL base solution containing 0.5 mol/L NaOH and 0.1 mol/L Na_2CO_3 were first prepared. These solutions are then simultaneously added dropwise to a 2 L beaker (initially containing 200 mL of ultrapure water) using an automatic pH dosing machine (Kroma CPH-2). The reaction was conducted under continuous magnetic stirring and a pH of 8 ± 0.1.

https://doi.org/10.1180/mgm.2024.61 Published online by Cambridge University Press

After that, the mixture was stirred for an additional 2 hours and then left to age for 12 hours. Following aging, the solid was collected by centrifugation and washed by ultrapure water until the supernatant reached near-neutral pH. Then the product was separated and dried to obtain the CoAl-LDH. As for the synthesis of NiFe-LDH, the procedures keep the same with the synthesis of CoAl-LDH, with the difference of using $Ni(NO_3)_2 \cdot 6H_2O$ and $Fe(NO_3)_3 \cdot 9H_2O$ to replace $Co(NO_3)_2 \cdot 6H_2O$ and $Al(NO_3)_3 \cdot 9H_2O$, respectively.

2.2 Alternating oxidation and reduction of LDH

Sodium borohydride and hydrogen peroxide were selected to carry out the oxidation-reduction reaction on CoAl-LDH and NiFe-LDH. For CoAl-LDH, a certain amount of CoAl-LDH was placed in a beaker, and hydrogen peroxide solution (mass ratio of 30%) was added in the beaker with a ratio of 1 g LDH per 20 mL of hydrogen peroxide solution. The reaction was stirred for 30 minutes to oxidize the divalent cobalt ions in CoAl-LDH. After oxidation, the product was washed with ultrapure water and dried. The resulting product is the first oxidation product of CoAl-LDH; the product hereafter is named as CoAl-LDH-FO (FO: first oxidized). After that, CoAl-LDH-FO was reduced by sodium hydroxide to generate the first reduction product CoAl-LDH-FR. The procedure is as follow: a certain amount of the CoAl-LDH-FO was put into a beaker which contains sodium hydroxide solution (pH 10) with a solid-liquid ratio of 1 g : 20 mL. Then, borohydride sodium was added in the beaker with a ratio of 1 g LDH to 100 mg of borohydride sodium, and the solution was stirred for 30 minutes to reduce the metal ions of Co(III). After reduction, the product (CoAl-LDH-FR) was washed

https://doi.org/10.1180/mgm.2024.61 Published online by Cambridge University Press

three times with ultrapure water and dried. Repeat the above alternating oxidation and reduction processes to obtain the second oxidized and second reduced products CoAl-LDH-SO and CoAl-LDH-SR. That is, the original CoAl-LDH underwent the "first oxidation-first reduction-second oxidation-second reduction" process.

The oxidation-reduction evolution of NiFe-LDH is similar to the above process, with the difference being the reduction reaction happened first and followed by the oxidation reaction. That is, NiFe-LDH underwent "first reduction-first oxidation-second reduction-second oxidation" to generate products of NiFe-LDH-FR, NiFe-LDH-FO, NiFe-LDH-SR, and NiFe-LDH-SO in turn.

In order to reveal the leaching of heavy metals from LDH during REDOX process, concentrations of the heavy metals in the solution generated from each evolution process as well as the heavy metal contents in the original LDH were determined by ICP-MS (7900, Agilent).

2.3 Determination of ratio of Co(II)/Co(III) and Fe(II)/Fe(III)

Co(II)/Co(III) and Fe(II)/Fe(III) ratios were determined after each oxidation or reduction process. All the CoAl-LDH and NiFe-LDH were dissolved by HCl to obtain Co and Fe solution. Then, Co(II) detection was conducted by Nitroso-R salt spectrophotometric method (Yu et al., 2024). In detail, in sodium acetate (pH 5.5–6.0) solution, Co(II) ions can react with nitroso-R salt (also known as NRS) to form soluble red complexes; the concentration of this red complexes can be determined at 530 nm by using a UV/VIS spectrophotometer. The concentration of Fe(II) was detected by the 1,10-phenanthroline method (Liang et al., 2019). The total amounts of Co and Fe in

https://doi.org/10.1180/mgm.2024.61 Published online by Cambridge University Press

LDH were detected by ICP-MS as stated in Section 2.2. Finally, the ratios of Co(II)/Co(III) and Fe(II)/Fe(III) can be obtained via above procedures.

2.4 Testing of metal occurrence forms in LDH

Metals (Ni, Fe, Co and Al) in the original, oxidized, and reduced LDH were extracted using the Tessier method to determine their occurrence forms (Tessier et al., 1979). First step: 2 g of each LDH was put in 25 mL centrifuge tube, and then 16 mL of 1 mol/L $MgCl_2$ (pH=7) was added in the tube. The reaction lasted for 1 h at room temperature under oscillation. After oscillation, centrifugation was carried out at 4000 rpm for 10 minutes, and the supernatant was collected for heavy metal concentration test and the solid was used for the following experiments. Second step: 16 mL of 1 mol/L NaAc (pH=5.5, adjusted by HAc) was added into the tube which contained the residual solid of first step. The reaction lasted for 5 h at room temperature under oscillation. After oscillation, centrifugation was done for 10 minutes. The supernatant was collected for heavy metal concentration test and the solid was used for third step. Third step: the resulting solid from second step was dried and digested, and the heavy metal concentration was measured using ICP-MS after dilution. Each experiment was repeated twice. As the used LDH does not contain organic matter and iron-manganese oxides, we mainly determined exchangeable, carbonate bounded, and residual forms of metals.

2.5 Cd adsorption experiment

The adsorption of Cd^{2+} was used to evaluate the effect of alternating oxidation-reduction evolution on the surface adsorption reactivity of LDH, and further to estimate

https://doi.org/10.1180/mgm.2024.61 Published online by Cambridge University Press

whether oxidation-reduction evolution would cause the re-migration of surface-adsorbed heavy metals on LDH. Batch adsorption experiments were conducted to determine the isothermal adsorption behavior. The adsorption experiments were carried out in glass tube with cover, with an adsorbent addition of 1 g/L. The Cd^{2+} concentration ranging from 5-100 mg/L. The reactions were conducted for 12 h under pH of 7, 25°C, and oscillation. After adsorption, centrifugation was performed, and the Cd^{2+} concentration in the supernatant was measured by ICP-MS.

2.6 Characterization methods

X-ray diffraction analysis (XRD) of the products were measured on a Bruker D8 ADVANCE X–ray diffractometer using Cu Kα radiation operating at 40 kV and 40 mA. The patterns were recorded over the 2θ range from 3 to 80° with a scan speed of 3°/min using a bracket sample holder. XRD primarily served to determine whether LDH structure was destroyed after the redox reaction. SEM images were obtained by Gemini SEM 460 (ZEISS) high-resolution field emission scanning electron microscopy. Zeta potential test was primarily used to measure the charge state of LDH. Variation of Zeta potential with pH of the products was detected by Malvern Zetasizer Nano-ZS (Malvern Instruments, UK). 1 mmol/L $NaNO_3$ was used as electrolyte solution during the measurements (Liu et al., 2018), and all the measurements were accomplished at room temperature.

3. Results and discussion

3.1 Effects of redox evolution on the structural and surface characteristics of LDH

XRD results show that there is no significant phase change between the original

https://doi.org/10.1180/mgm.2024.61 Published online by Cambridge University Press

CoAl-LDH and its first oxidized sample (CoAl-LDH-FO), but the d(003) value of the CoAl-LDH-FO (0.890 nm) is reduced by c.a. 0.02 nm compared with that of the original CoAl-LDH (0.871 nm) (Figure 1a). This is because the structural Co(II) (ionic radius 74.5 pm) is oxidized to Co(III) (ionic radius 54.5 pm); the reduction of ionic radius caused a shift to a higher diffraction angle (Deng et al., 2018). The subsequent redox reaction would completely destroy LDH structure resulting in the formation of amorphous products (CoAl-LDH-FR, CoAl-LDH-SO, and CoAl-LDH-SR) indicated by the disappearance of all diffraction peaks. Guo et al. also indicated that the oxidation of Co^{2+} to Co^{3+} in NiCo-LDH would result in the disappearance of the characteristic diffraction peaks of the layered structure (Gou et al., 2016). Therefore, the disappearance of characteristic diffraction peaks of LDH herein should be due to the change of valence state of Co. As for NiFe-LDH, XRD results indicate that there is no significant phase change before and after oxidative-reductive alternating evolution, but the oxidative-reductive alternating evolution affected the order degree of LDH nano plate on the c-axis (Figure 1b).

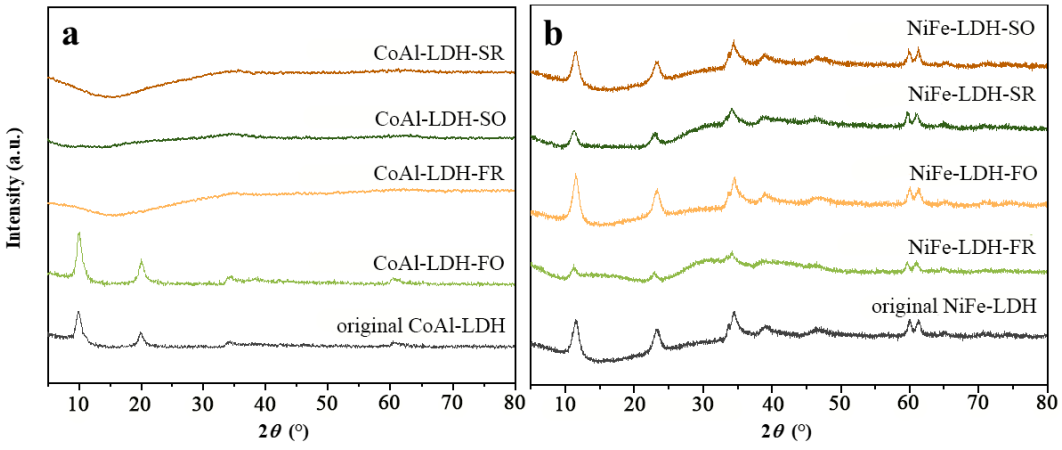

Figure 1. XRD patterns of the original, oxidized, and reduced LDH: (a) CoAl-LDH and its oxidized and reduced products; (b) NiFe-LDH and its oxidized and reduced products.

https://doi.org/10.1180/mgm.2024.61 Published online by Cambridge University Press

Zeta potential test results showed that original LDH and the oxidized and reduced products all have positively charged surface (Figure 2), indicating that the sample may still retain part of the LDH structure after oxidation and reduction. As the amount of positive charge of LDH is depended on the content of structural metal in higher valence state, destruction of layered structure of LDH would alter the content of structural metals and thus change the surface charge of LDH (Laipan et al. 2020). For CoAl-LDH, after the first oxidation, the surface charge in pH 7-10 (from 26~24 mV) is higher than the original one (from 25.2~22.5 mV), indicating that oxidation will not destroy the LDH structure, well in agreement with the XRD results. The reason for the increase of the charge may be that the first oxidation promotes the integrity of LDH structure (Figure 1a). However, the subsequent reduction and oxidation significantly reduced the surface charge of the products (decrease from 28~18 mV to 3~0.5 mV in pH range of 5-11), indicating that the subsequent treatment will significantly destroy the structure of LDH, which is consistent with the XRD results. As for NiFe-LDH, the zeta potential test results demonstrated that the oxidative-reductive evolution also has a significant impact on the structure of NiFe-LDH. But unlike CoAl-LDH, the oxidation and reduction led to an increase of the positive charge of NiFe-LDH (mostly increase from 1.5~0.6 mV to 3.25~0.75 mV in pH range of 5-11, Figure 2b), indicating that the reduced and oxidized products of NiFe-LDH may retain the LDH structure after multiple oxidative-reductive treatments, well in agreement with the XRD results. The increase in positive charge content also indicates that there are certain changes in the proportion and occupancy of Ni and Fe in the structural layers of NiFe-LDH, possibly

https://doi.org/10.1180/mgm.2024.61 Published online by Cambridge University Press

due to the detachment of some Ni(II) from the structural layers of LDH during the oxidative-reductive evolution (please see Figure 4b below), leading to a higher proportion of Fe^{3+} in the products compared to the original sample. This inference is based on the fact that the amount of structural charge of LDH depends mainly on the content of structural metal element with higher oxidation state (Yu et al. 2017, Laipan et al. 2020). Additionally, previous study also indicated that Ni^{2+} can be oxidized to Ni^{3+} (Zhao et al., 2015, Liu et al., 2017), thus amount of positive charge of LDH layers increased.

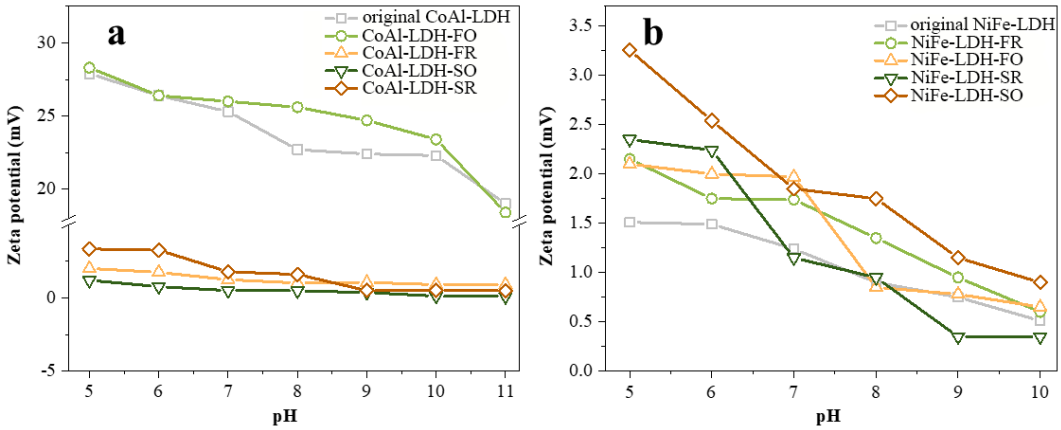

Figure 2. Variation of Zeta potential of the original, oxidized, and reduced LDH: (a) CoAl-LDH and its oxidized and reduced products; (b) NiFe-LDH and its oxidized and reduced products.

SEM images also suggested the destruction or preservation of LDH structure of the reduced and oxidized LDH (Figure 3). For CoAl-LDH, the sheet-like morphology was destroyed markedly by redox evolution, and the sheets were transferred to dense blocks as redox evolution progresses. This result indicates the destruction of CoAl-LDH structure, well in agreement with XRD results. As indicated by XRD results, CoAl-LDH-FO and CoAl-LDH showed similar diffraction peaks with comparable diffraction intensity; therefore CoAl-LDH-FO should have similar morphology with CoAl-LDH. SEM image of CoAl-LDH-FO in Figure 3 fits well with the above

https://doi.org/10.1180/mgm.2024.61 Published online by Cambridge University Press

reasoning. As reduction and oxidation proceed, the sheets were transferred to dense blocks. As for NiFe-LDH, the redox evolution showed little effect on the flake morphology, indicating that the structure of LDH was not obviously affected, also well in agreement with XRD results. In summary, compared to CoAl-LDH, the structure of NiFe-LDH is more stable, and the oxidative-reductive process did not cause significant damage to its structure.

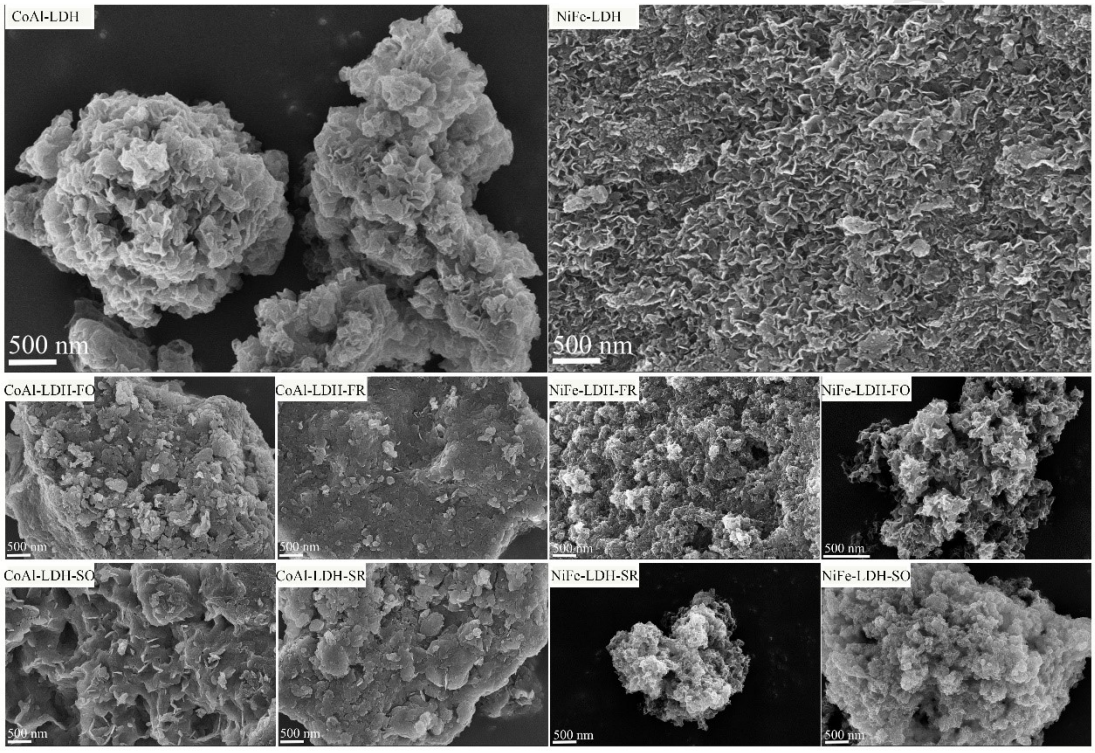

Figure 3. Variation of morphology of the original, oxidized, and reduced CoAl-LDH and NiFe-LDH.

3.2 Impact of redox evolution on the transfer and occurrence of heavy metals

Each redox evolution caused 24.4%-93.5% of Co or Fe in CoAl-LDH and NiFe-LDH to be reduced or oxidized (Table 1), which suggested CoAl-LDH and NiFe-LDH could be partially reduced or oxidized. Leaching results of heavy metals indicates that c.a. 2%-3% of Co and Ni would transfer from LDH structure to solution after all the oxidation-reduction alternating evolution process (Figure 4). Each oxidation or

https://doi.org/10.1180/mgm.2024.61 Published online by Cambridge University Press

reduction resulted in the dissolution of heavy metals, and oxidation process contributed to the transfer of heavy metals more significantly than reduction process (0.8%-1.3% for each oxidation process and 0.06%-0.16% for each reduction process). The redox evolution also greatly affected the occurrence forms of heavy metal ions. The percentages of exchangeable, carbonate-bounded, and residual forms of metal elements in the original LDH and their oxidative-reductive evolution products were determined through leaching experiments (Figure 5). The results indicated that the contents of exchangeable and carbonate-bounded forms of the metals are relatively low, while the content of the residual state is high, indicating that both LDH have a strong ability to lock heavy metal ions. For original CoAl-LDH, the content of exchangeable (5.48%) and carbonate-bounded Co (46.30%) indicated that a half of Co did not enter the LDH structure. The low proportion of residual Al (66.11%) and high carbonate-bounded Al (33.89%) also suggested a third of the Al was not involved in the formation of CoAl-LDH. These results indicated that the original CoAl-LDH is a mixture of metal carbonate and LDH. It can be seen that after multiple cycles of oxidative-reductive evolution, the carbonate-bounded Co and Al significantly transformed into the residual state (increased from 66.11% to 99.05% for Al, and 48.22% to 87.22% for Co), indicating that redox evolution contributed to a more stable state of heavy metal. This result demonstrated that the redox evolution of CoAl-LDH would result in a more secure fixation of Co and a significant reduction in its bioavailability.

https://doi.org/10.1180/mgm.2024.61 Published online by Cambridge University Press

Table 1. Redox ratio of Co and Fe in each redox reaction

Sample	Total Co or Fe (mg/g)	Co(II) or Fe(II) (mg/g)	Co(III) or Fe(III) (mg/g)	Co(II)/Co(III) or Fe(II)/Fe(III)	redox ratio (%)
			Co		
CoAl-LDH	370.7	368.3	2.4	153.5	–
CoAl-LDH-FO	367.0	277.5	89.5	3.1	24.4
CoAl-LDH-FR	366.6	360.8	5.8	62.2	93.5
CoAl-LDH-SO	361.5	205.7	155.8	1.3	43.0
CoAl-LDH-SR	360.9	338.1	22.8	14.8	85.4
			Fe		
NiFe-LDH	174.8	0.0	174.8	0.0	–
NiFe-LDH-FR	171.3	64.8	106.5	0.6	37.1
NiFe-LDH-FO	171.2	11.5	159.7	0.1	82.3
NiFe-LDH-SR	166.7	92.3	74.4	1.2	53.4
NiFe-LDH-SO	166.8	7.4	159.4	0.0	92.0

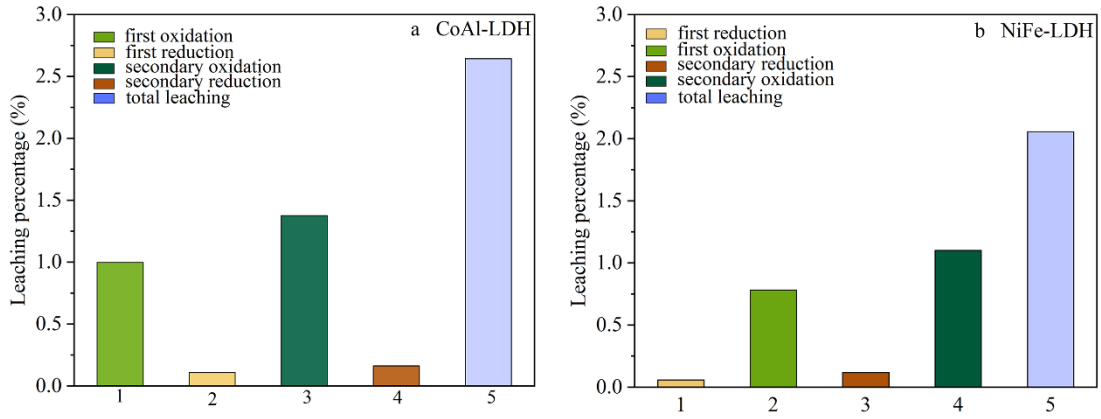

Figure 4. Leaching percentage of heavy metals during oxidation-reduction alternating evolution process: (a) leaching of Co in CoAl-LDH; (b) leaching of Ni in NiFe-LDH. Co content in the original CoAl-LDH is 370.7 mg/g LDH; Ni content in the original NiFe-LDH is 345.2 mg/g LDH.

As for NiFe-LDH, redox evolution caused a gradual decrease of carbonate-bounded Fe (from 3.91% to 0), and a slight increase of residual form of Fe (from 96.09% to 99.50%, Figure 5c). Meanwhile, redox evolution led to a decrease of exchangeable Ni (from 4.53% to 1.85%) and a slight increase of residual form of Ni (from 79.51% to 87.63%, Figure 5d). But reduction would result in the increase of carbonate-bounded Ni (from 15.96% to 24.82%), while oxidation caused a contrary tendency. Overall,

https://doi.org/10.1180/mgm.2024.61 Published online by Cambridge University Press

redox evolution can also result in a more secure fixation of Ni and a reduction in its bioavailability.

Combining the above results, it can be concluded that redox evolution leads to a tighter binding of heavy metal ions with the LDH structure or solid phase, resulting in a decrease in the content of bioavailable heavy metals. But it will also cause a small amount of heavy metal to transfer from solid phase to liquid phase during redox process.

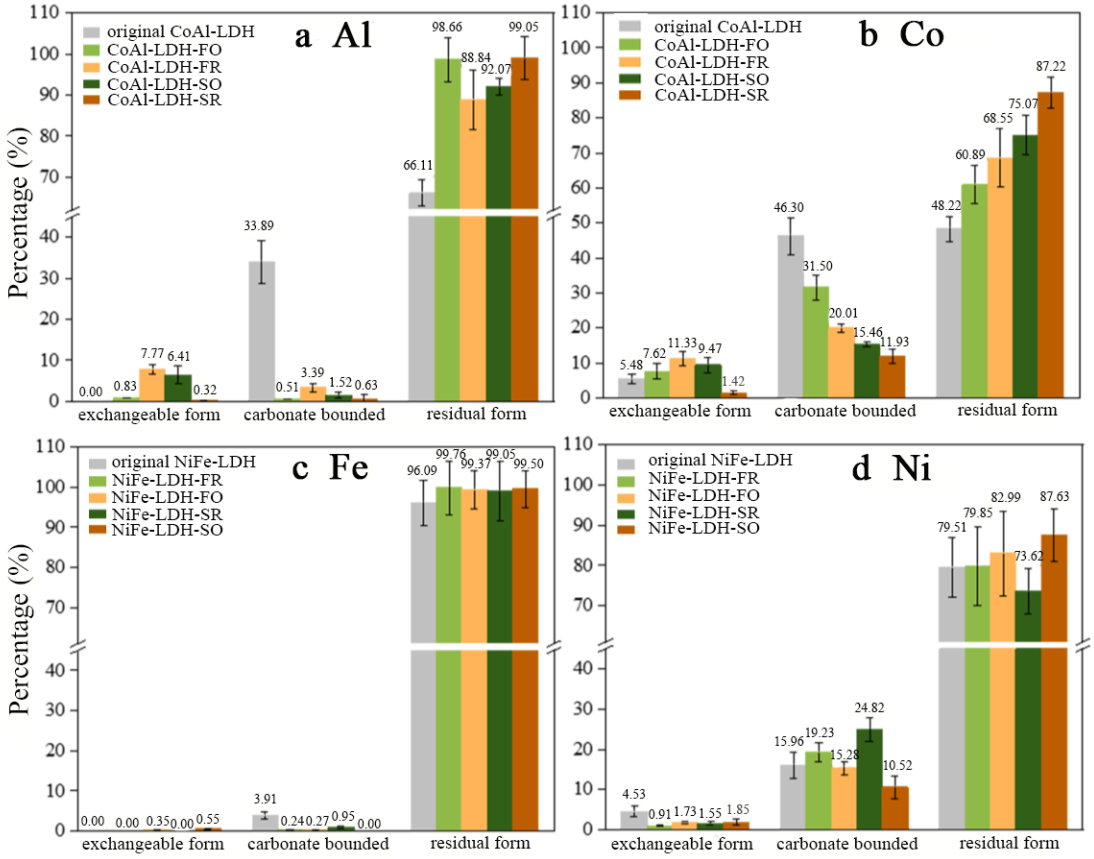

Figure 5. Occurrence forms of Al, Co, Fe, and Ni in the original, oxidized, and reduced LDH: (a) Al in CoAl-LDH; (b) Co in CoAl-LDH; (c) Fe in NiFe-LDH; (d) Ni in NiFe-LDH.

3.3 Impact of redox evolution on the adsorptive ability of LDH

The redox evolution of LDH affected not only the locking performance of heavy metal ions in their structure but also their adsorption ability for fixing heavy metal ions. The Cd(II) adsorption isotherms of CoAl-LDH, FeNi-LDH, and their oxidized and reduced products indicated that the redox evolution significantly decreased the

https://doi.org/10.1180/mgm.2024.61 Published online by Cambridge University Press

adsorption capacity of LDH (Figure 6). For the original CoAl-LDH and its first oxidation product, they showed comparable adsorption performance to Cd(II) with maximum adsorption capacities of c.a. 14 and 12 mg/g. This result should be due to their similar LDH structure, morphology, and zeta potential in pH 7 (Figure 1~3). The subsequent oxidative or reductive evolution strongly weakened the adsorption ability of LDH (decrease from c.a. 14 to 1 mg/g of the maximum adsorption capacity, Figure 6a), which should be mainly resulted from the destruction of LDH structure and formation of a denser aggregation of sheets and dense blocks (Figure 1 and 3). As for NiFe-LDH, similar results were observed. The original NiFe-LDH exhibited the best adsorption performance for Cd(II), and the subsequent oxidative-reductive evolution greatly reduced the adsorption performance (decrease from c.a. 13 to 6 mg/g of the maximum adsorption capacity, Figure 6b). The combination of variation of layered structure and decrease of zeta potential may be the main reason for the decrease of adsorptive ability (Figure 1 and 2). Considering the above experimental results, it can be concluded that the oxidative-reductive evolution is not conducive to LDH exerting a fixation effect on surrounding heavy metal ions.

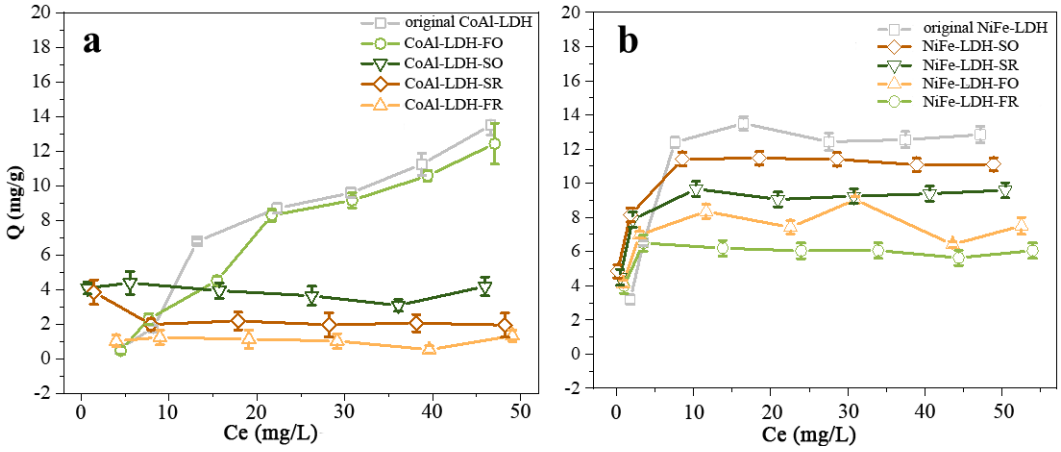

Figure 6. Variation of adsorptive performance to Cd(II) of the CoAl-LDH and NiFe-LDH after

https://doi.org/10.1180/mgm.2024.61 Published online by Cambridge University Press

oxidation-reduction alternating evolution: (a) CoAl-LDH and its oxidized and reduced products; (b) NiFe-LDH and its oxidized and reduced products.

3.4 The relationship between the variation of structure characteristics and the fixation performance of heavy metals

As mentioned earlier, for CoAl-LDH, the alternating oxidative-reductive evolution caused the disappearance of all characteristic diffraction peaks belonging to LDH after multiple oxidation and reduction cycles, the positive charge content of the structure significantly decreases (from 20-27 mV to 0-5 mV), and the sheet-like morphology of LDH was remarkably destroyed. These results indicated that the oxidative-reductive evolution led to significant structural damage to CoAl-LDH. The structural damage resulted in a significant change in the occurrence form of heavy metal cobalt ions in the structure. In detail, the structural damage caused some cobalt ions to transform into an exchangeable form, and with the progression of the oxidative-reductive evolution, the exchangeable content gradually increased, suggesting an increase in the most bioavailable form. However, from Figure 5b, it can be seen that the exchangeable cobalt mainly comes from the transformation of the carbonate-bounded state. At the same time, after the oxidative-reductive evolution, most of the carbonate-bounded state transformed into the residual state. Overall, the content of bioavailable heavy metals (exchangeable and carbonate-bounded states) gradually decreases with the progression of the oxidative-reductive evolution. However, considering the evolution of the CoAl-LDH structure, the increase in the content of residual state heavy metals is positively correlated with the structural damage of LDH, indicating that the increase in the residual state may be due to the formation of cobalt oxides and/or

https://doi.org/10.1180/mgm.2024.61 Published online by Cambridge University Press

hydroxides. Additionally, the evolution (damage) of the structure significantly reduced the purification ability of CoAl-LDH for surrounding heavy metal ions. The adsorption activity of a LDH for heavy metal ions mainly originated from structural hydroxyl groups, isomorphic substitution, and the availability of interlayer ions (Liang et al. 2013, He et al. 2018, Laipan et al. 2023). The structural damage of LDH would lead to a significant reduction in the content of structural hydroxyl groups, the number of octahedral vacancies in the LDH structure, and the content of interlayer anion active sites (Yang et al., 2002). These should be the reasons for the significant decrease in the adsorption capacity for heavy metals of CoAl-LDH after redox evolution.

For NiFe-LDH, as analyzed earlier, the oxidative-reductive evolution did not cause significant damage to the LDH structure; instead, it helped the growth of LDH crystals. The oxidative-reductive evolution to some extent sharpens the diffraction peaks belonging to LDH (Figure 1), and the structural charge increases (Figure 2), indicating that the evolution contributed to the formation of the LDH structure. The improvement of LDH structure and increase of structure charge led to a decrease in the content of exchangeable heavy metals and an increase in the content of the residual state. In an open system, the formation and growth of a LDH can promote the conversion of carbon dioxide in the air into carbonate ions, which then enter the interlayers of LDH as balancing anions (Laipan et al., 2018, Laipan et al. 2023). This may be the reason for the increase in the content of carbonate-bounded state heavy metals during evolution. This also reflects that the oxidative-reductive evolution contributes to the improvement of the NiFe-LDH structure. Similar to CoAl-LDH, the oxidative-reductive evolution

https://doi.org/10.1180/mgm.2024.61 Published online by Cambridge University Press

helps to more securely lock the heavy metal ions in the LDH structure. However, the redox evolution also caused the decrease of adsorptive ability of NiFe-LDH for surrounding heavy metals. The increase in surface positive charge may be an important reason for the decrease in its adsorption capacity. The electrostatic repulsion to some extent inhibits the contact of Cd(II) with the LDH surface. Overall, the fixation performance of LDH for heavy metal ions in the structure and the surrounding environment is closely related to its structural evolution.

4. Conclusion

This study investigated the influence of the change in metal oxidation states of the structural metal compositions of LDH on the migration and transformation of structural and surface-adsorbed heavy metals, as well as the surface reactivity of LDH toward surrounding heavy metals. The results indicated that the oxidative-reductive alternating evolution of LDH constrained the transformation of heavy metals, as well as their bioavailability greatly. On the one hand, the alternating oxidative-reductive evolution helps LDH to reduce the content of bioavailable heavy metals such as exchangeable and carbonate-bounded states, and makes the binding of heavy metal ions to LDH more firmly. The alternating oxidative-reductive evolution promoted the transformation of exchangeable and carbonate-bounded heavy metals into residual state, reducing their mobility and bioavailability. Therefore, the alternating oxidative-reductive evolution enhanced LDH's ability in the locking of its structural heavy metal ions. On the other hand, the oxidative-reductive evolution of LDH reduced their surface adsorption ability of surrounding heavy metals, thereby reducing their interfacial locking capacity for

https://doi.org/10.1180/mgm.2024.61 Published online by Cambridge University Press

surrounding heavy metal ions. In the long run, this may reduce the environmental purification performance of LDH for surrounding contaminants.

Conflicts of interest

There are no conflicts to declare.

Acknowledgment

M. Laipan thanks the financial support from National Natural Science Foundation of China (41902039) and Natural Science Basic Research Program of Shaanxi Province (2024JC-YBQN-0319). J. Guo thanks the financial support from the Shaanxi Province Science and Technology Innovation Team (2022TD-09) and the Key Industrial Chain Project of Shaanxi Province (2022ZDLNY02-02).

Author Contributions

Mengyao Yuan performed the experiment and wrote the manuscript. Minwang Laipan conceived and designed the experiments, analyzed the data, and edited the manuscript. Min Zhang, Xueya Wan, and Ziyu Wang performed the characterization section. Junkang Guo edited the manuscript.

References

Ahmad, N. N. R., W. L. Ang, Y. H. Teow, A. W. Mohammad and N. Hilal (2022). "Nanofiltration membrane processes for water recycling, reuse and product recovery within various industries: A review." Journal of Water Process Engineering **45**: 102478.

Aucour, A.-M., J.-P. Bedell, M. Queyron, V. Magnin, D. Testemale and G. Sarret (2015). "Dynamics of Zn in an urban wetland soil-plant system: Coupling isotopic and EXAFS approaches." Geochimica Et Cosmochimica Acta **160**: 55-69.

de Souza E Silva, P. T., N. T. de Mello, M. M. Menezes Duarte, M. C. B. S. M. Montenegro, A. N. Araujo, B. de Barros Neto and V. L. da Silva (2006). "Extraction and recovery of chromium from electroplating sludge." Journal of hazardous materials **128**(1): 39-43.

Deng, L., H. Zeng, Z. Shi, W. Zhang and J. Luo (2018). "Sodium dodecyl sulfate intercalated and acrylamide anchored layered double hydroxides: A multifunctional adsorbent for highly efficient removal of Congo red." Journal of colloid interface science **521**: 172-182.

https://doi.org/10.1180/mgm.2024.61 Published online by Cambridge University Press

Gou, J., S. Xie, Y. Liu and C. Liu (2016). "Flower-like nickel-cobalt hydroxides converted from phosphites for high rate performance hybrid supercapacitor electrode materials." Electrochimica Acta **210**: 915-924.

Guo, J., L. Wang, Y. Tu, H. Muhammad, X. Fan, G. Cao and M. Laipan (2021). "Polypyrrole modified bentonite nanocomposite and its application in high-efficiency removal of Cr (VI)." Journal of Environmental Chemical Engineering **9**(6): 106631.

Guo, J., J. Zhao, X. Ren, H. Jia, H. Muhammad, X. Lv, T. Wei and L. Hua (2020). "Effects of Burkholderia sp. D54 on growth and cadmium uptake of tomato, ryegrass and soybean plants." International journal of environmental science technology **17**: 1149-1158.

Haris, M., Y. Hamid, L. Wang, M. Wang, N. Yashir, F. Su, A. Saleem, J. Guo and Y. Li (2022). "Cd diminution through microbial mediated degraded lignocellulose maize straw: Batch adsorption and bioavailability trails." Journal of Environmental Management **302**: 114042.

He, X., X. Qiu, C. Hu and Y. Liu (2018). "Treatment of heavy metal ions in wastewater using layered double hydroxides: A review." Journal of Dispersion Science and Technology **39**(6): 792-801.

Laipan, M., Q. Chen, Z. Wang, M. Zhang, M. Yuan, R. Zhu and L. Sun (2023). "Interlayer Anions of Layered Double Hydroxides as Mobile Active Sites To Improve the Adsorptive Performance toward Cd2+." Inorganic Chemistry **62**(34): 13857-13866.

Laipan, M., H. Fu, R. Zhu, L. Sun, R. M. Steel, S. Ye, J. Zhu and H. He (2018). "Calcined Mg/Al-LDH for acidic wastewater treatment: Simultaneous neutralization and contaminant removal." Applied Clay Science **153**: 46-53.

Laipan, M., J. Yu, R. Zhu, J. Zhu, A. T. Smith, H. He, D. O'Hare and L. Sun (2020). "Functionalized layered double hydroxides for innovative applications." Materials Horizons **7**(3): 715-745.

Laipan, M., M. Zhang, Z. Wang, R. Zhu and L. Sun (2024). "Highly efficient recovery of Zn2+/Cu2+ from water by using hydrotalcite as crystal seeds." The Science of the total environment **914**: 169954-169954.

Liang, X., Y. Li, G. Wei, H. He, J. W. Stucki, L. Ma, L. Pentrakova, M. Pentrak, J. J. A. E. Zhu and S. Chemistry (2019). "Heterogeneous reduction of 2-chloronitrobenzene by co-substituted magnetite coupled with aqueous Fe2+: Performance, factors, and mechanism." ACS Earth and Space Chemistry **3**(5): 728-737.

Liang, X., Y. Zang, Y. Xu, X. Tan, W. Hou, L. Wang and Y. Sun (2013). "Sorption of metal cations on layered double hydroxides." Colloids and Surfaces A: Physicochemical and Engineering Aspects **433**: 122-131.

Liu, J., R. L. Zhu, T. Y. Xu, M. W. Laipan, Y. P. Zhu, Q. Zhou, J. X. Zhu and H. P. He (2018). "Interaction of polyhydroxy fullerenes with ferrihydrite: adsorption and aggregation." Journal of Environmental Sciences **64**: 1-9.

Liu, Q., H. Wang, X. Wang, R. Tong, X. Zhou, X. Peng, H. Wang, H. Tao and Z. Zhang (2017). "Bifunctional Ni 1− x Fe x layered double hydroxides/Ni foam electrodes for high-efficient overall water splitting: a study on compositional tuning and valence state evolution." International Journal of Hydrogen Energy **42**(8): 5560-5568.

Liu, X., M. Laipan, C. Zhang, M. Zhang, Z. Wang, M. Yuan and J. Guo (2024). "Microbial weathering of montmorillonite and its implication for Cd (II) immobilization." Chemosphere **349**: 140850.

Liu, Z., Z. Xu, L. Xu, F. Buyong, T. C. Chay, Z. Li, Y. Cai, B. Hu, Y. Zhu and X. Wang (2022). "Modified biochar: synthesis and mechanism for removal of environmental heavy metals." Carbon Research **1**(1): 8.

https://doi.org/10.1180/mgm.2024.61 Published online by Cambridge University Press

Muhammad, H., T. Wei, G. Cao, S. Yu, X. Ren, H. Jia, A. Saleem, L. Hua, J. Guo and Y. Li (2021). "Study of soil microorganisms modified wheat straw and biochar for reducing cadmium leaching potential and bioavailability." Chemosphere **273**: 129644.

Peltier, E., D. van der Lelie and D. L. Sparks (2010). "Formation and Stability of Ni-Al Hydroxide Phases in Soils." Environmental Science & Technology **44**(1): 302-308.

Qiu, M., L. Liu, Q. Ling, Y. Cai, S. Yu, S. Wang, D. Fu, B. Hu and X. Wang (2022). "Biochar for the removal of contaminants from soil and water: a review." Biochar **4**(1): 19.

Siebecker, M. G., W. Li and D. L. Sparks (2018). The Important Role of Layered Double Hydroxides in Soil Chemical Processes and Remediation: What We Have Learned Over the Past 20 Years. Advances in Agronomy, vol 147. **147:** 1-59.

Sodango, T. H., X. Li, J. Sha and Z. Bao (2018). "Review of the spatial distribution, source and extent of heavy metal pollution of soil in China: impacts and mitigation approaches." Journal of Health Pollution **8**(17): 53-70.

Tessier, A., P. G. Campbell and M. Bisson (1979). "Sequential extraction procedure for the speciation of particulate trace metals." Analytical chemistry **51**(7): 844-851.

Wang, B., F. Liu, F. Zhang, M. Tan, H. Jiang, Y. Liu and Y. Zhang (2022a). "Efficient separation and recovery of cobalt(II) and lithium(I) from spent lithium ion batteries (LIBs) by polymer inclusion membrane electrodialysis (PIMED)." Chemical Engineering Journal **430**: 132924.

Wang, L., M. Wang, H. Muhammad, Y. Sun, J. Guo and M. Laipan (2022b). "Polypyrrole-Bentonite composite as a highly efficient and low cost anionic adsorbent for removing hexavalent molybdenum from wastewater." Journal of Colloid Interface Science **615**: 797-806.

Xu, M., J. Ma, X.-H. Zhang, G. Yang, L.-L. Long, C. Chen, C. Song, J. Wu, P. Gao and D.-X. Guan (2023). "Biochar-bacteria partnership based on microbially induced calcite precipitation improves Cd immobilization and soil function." Biochar **5**(1): 20.

Yang, W., Y. Kim, P. K. Liu, M. Sahimi and T. T. Tsotsis (2002). "A study by in situ techniques of the thermal evolution of the structure of a Mg–Al–CO3 layered double hydroxide." Chemical Engineering Science **57**(15): 2945-2953.

Yu, J., Q. Wang, D. O'Hare and L. Sun (2017). "Preparation of two dimensional layered double hydroxide nanosheets and their applications." Chemical Society Reviews **46**: 5950-5974.

Yu, T., W. Zhou, Y. Zhang, Y. Fang, Y. J. S. Cheng and P. Technology (2024). "Molecular dynamics simulation study on the interaction mechanisms of leaching solutions and LiCoO2 surface." Separation and Purification Technology **339**: 126596.

Zhang, Y., M. Haris, L. Zhang, C. Zhang, T. Wei, X. Li, Y. Niu, Y. Li, J. Guo and X. Li (2022). "Amino-modified chitosan/gold tailings composite for selective and highly efficient removal of lead and cadmium from wastewater." Chemosphere **308**: 136086.

Zhao, Y., Q. Wang, T. Bian, H. Yu, H. Fan, C. Zhou, L.-Z. Wu, C.-H. Tung, D. O'Hare and T. Zhang (2015). "Ni 3+ doped monolayer layered double hydroxide nanosheets as efficient electrodes for supercapacitors." Nanoscale **7**(16): 7168-7173.

Zhou, J. Z., Y. Y. Wu, C. Liu, A. Orpe, Q. Liu, Z. P. Xu, G. R. Qian and S. Z. Qiao (2010). "Effective Self-Purification of Polynary Metal Electroplating Wastewaters through Formation of Layered Double Hydroxides." Environmental Science & Technology **44**(23): 8884-8890.

Zhu, R., Q. Chen, Q. Zhou, Y. Xi, J. Zhu and H. He (2016). "Adsorbents based on montmorillonite for contaminant removal from water: A review." Applied Clay Science **123**: 239-258.

Zhu, Y. and E. J. Elzinga (2014). "Formation of Layered Fe(II)-Hydroxides during Fe(II) Sorption onto

https://doi.org/10.1180/mgm.2024.61 Published online by Cambridge University Press

Clay and Metal-Oxide Substrates." Environmental Science & Technology **48**(9): 4937-4945.

https://doi.org/10.1180/mgm.2024.61 Published online by Cambridge University Press